Aalborg Universitet

AALBORG UNIVERSITY

DENMARK

Investigation of Acoustic Emission as a Non-invasive Method for Detection of Power Semiconductor Aging

P. Davari[a], O. Kristensen[a], F. Iannuzzo[a]

[a] Department of Energy Technology, Aalborg University, Aalborg, Denmark

Abstract

In this paper, recording of acoustic emission during real operations is used for non-invasively detecting the aging of a power module due to power cycling. The presented method is very simple and particularly attractive because of non-invasiveness and potential low-cost features, which can enable straightforward adoption in condition monitoring of power electronic devices. Nevertheless, a spectrum analysis is needed to process the acquired data. Experimental results show a strong correlation between acoustic emission and on-state voltage drop, which is the standard indicator of degradation in bond wires. A comparison with the results obtained with another identical module gave excellent repeatability, confirming that the method is very promising for real application.

1. Introduction

Power modules are the main component in converters for high power applications such as wind turbines, PV inverters, and traction applications. However, it has been shown that these components are some of the most susceptible to failures, causing failures of the full system [1]–[3]. For this reason, many research groups are presently working on condition monitoring, i.e. the possibility to acquire a number of parameter of operating power modules, in order to be able to detect their wear-out, and make timely maintenance.

Many proposal have been done so far to detect effectively wear-out in power modules. The most common approach is to measure the on-state voltage drop during operation [4]–[10]. This goal can be achieved in many different ways, but all of them require an auxiliary monitoring circuit connected directly to the module, based on instrumentation-class operational amplifiers. Several problems arise from this approach, though. First of all, being the device subjected to high voltage during off state, the monitoring circuit needs to be protected by means of e.g. a diode, which introduces an additional voltage to be accurately compensated with a periodical calibration. Second, the monitoring system needs galvanic isolation, as the module is not necessarily connected to the same reference voltage as the central monitoring unit. This galvanic isolation introduces, as a matter of fact, the need to convert the signal from analog to digital to pass through an opto-coupler or similar isolating transceiver, ending up in additional cost. Third, a failure in the monitoring unit itself can provoke failure in the power module, considerably reducing the overall reliability.

Recently, several papers have been presented about acoustic measurement methods [11]–[15]. Such methods have the big advantage to be contactless, which means that no electric contact is needed between the monitoring unit and the module under test, intrinsically solving all the problems of on-state voltage measurement. On the other hand, contactless methods need a higher complexity in decoding and correctly interpreting the monitored emission.

Acoustic emission has been proven to happen during a current switching, and claimed that it differs between a healthy power module and a failed power module in [12] and [14]. However, in these papers only the acoustic emission of an IGBT subject to short-circuit was investigated. In [15], though, it was shown that a variation can be observed in the acoustic emission of a power module when subjected to solder delamination. However, only the signal emitted during power cycling was measured, which is not
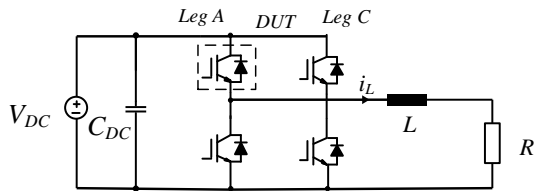
Figure 1. Electrical connections for the module under investigation.

necessarily the same as the one emitted in real operations.

In this work, it is investigated for the first time if aging can be detected by acoustic emission during an inductive switching in real operation of a power module. The correlation between acoustic emission and the degree of aging in the power module is investigated too, proving that it is possible to measure state of health by this method.

The paper is structured as follows: Section 2. describes the setup used for the tests. Section 3. illustrates the experimental procedure of the proposed method. Section 4. presents the obtained results and Section 5. deals with providing a repeatability proof of concept. Finally, conclusions are provided.

2. Setup description

An experimental setup has been built using a commercial 3-phase module rated at 1200 V and 25 A. (Danfoss PIM-E DP25F1200).

The module under test (MUT) contains, among other components not used in this study, 6 silicon IGBTs with anti-parallel diodes, arranged in three legs, namely A, B, and C. We have been using leg A and C only (see Figure 1). The load consists of an inductor with an inductance of 1 mH and a resistor with a resistance of 27 Ohm.

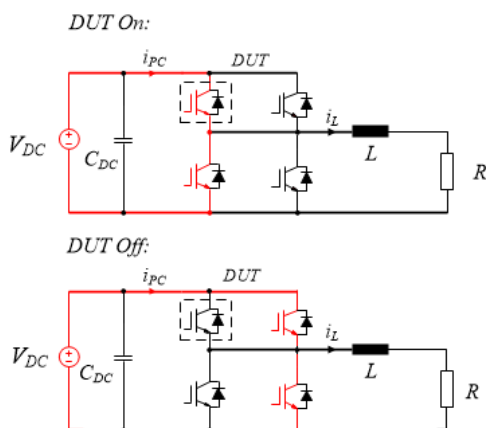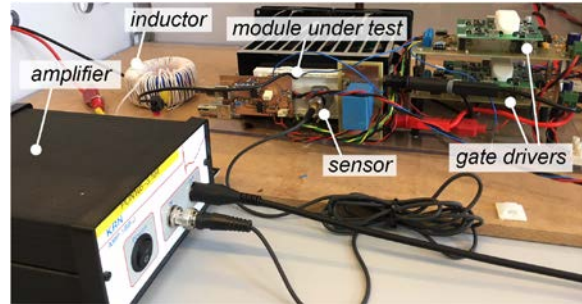The setup of Figure 1 has been designed in order to be

Figure 2. Setup used for investigation of acoustic emission.

operated in both power cycling mode and switching mode, as buck converter, without changing any connection, with the only exception of power supply. This feature is key to ensure that no artifact in the acoustic noise measurements can come from any change in surrounding things such as cable positioning, pressure force/between parts, and instrument-induced vibration. Two power supplies have been used, one for power cycling and the other for switching operation, which have been positioned on a separate table on top of one another, with cable connection stuck on the floor, in order to have no impact of the connection change on the setup.

To perform power cycling, the upper switch of phase-leg A is chosen as the Device Under Test (DUT) and its gate is pulsed at 0.5 Hz frequency together with the one of lower switch in the same leg. At the same time, the other leg is operated in interleaved mode, with a 100-microsecond overlap, in order to keep the V_{DC} power supply current constant while DUT is off (see Figure 3). IGBTs in phase-leg B are inhibited by connecting their gate terminals to their respective emitters. The current flowing through the L-R load is constant and very small with respect to the one

Figure 3. Connections during power cycling operation in the case of DUT on (top) and off (bottom).
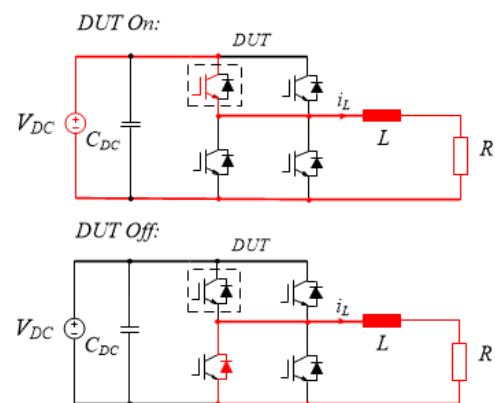

Figure 4. Connections during- switching operations in the case of DUT on (top) and off (bottom). Only DUT is operated, while the other three switches are held in off state.

through the DUT, so that it does not affect the power cycling operation. In this operating mode, the first V_{DC} power supply is set in current mode at 35 A. The DC-link voltage is very low, and corresponds to 2x IGBT on-state voltage drops.

To perform acoustic acquisition, the setup is operated in switching mode, in the same way it is supposed to work in the real case, with a switching frequency of 10 kHz. In this operating mode, the second V_{DC} power supply is set in voltage mode at 200 V. The drawn current is in the range of 2 – 3 Ampere.

Figure 2 displays a photograph of the used setup. One can recognize in it the module under test, mounted on a heat sink, a professional acoustic sensor KRNBB-PC, used for acoustic acquisition, and the gate driver boards on the right-hand side of the picture. A couple of fans are mounted on the back of the heatsink, which are kept on during acoustic emission measurements. Neither the oscilloscope Lecroy Wavesurfer 3024, nor the load bank and power supplies, Delta Elektronika SM 15-100 and SM 300-5, have been included in the figure for the sake of clarity. The resulting acoustic signals are recorded with the oscilloscope along with the switching signals, using a time window of 40 milliseconds and a sampling rate of 20 Megahertz. A sample acquisition is reported in Figure 5 with a time zoom of 300 microseconds. To determine whether a measurement of the same conditions yields the same acoustic emission, the measurement is repeated five
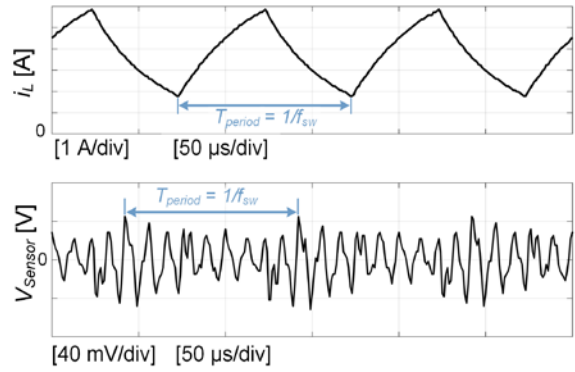
Figure 5. Sample oscilloscope acquisition. Inductor current (top) and the resulting acoustic signal (bottom) at 200 V and 10 kHz switching frequency.

times at the same stage.

3.   Experimental Procedure

The device under test has been characterized at fresh conditions first, by switching it at 200 V and its acoustic emission has been acquired. Afterwards, power cycling has been made. Initially, the power cycling was performed at 35 A. After 1000 cycles, this was increased to 45 A to further accelerate the aging. During this experiment, the power cycling was stopped at different instances and turned into switching mode in order to measure the acoustic

Figure 6. Conceptual schematic of the proposed acoustic measurement and device aging monitoring.

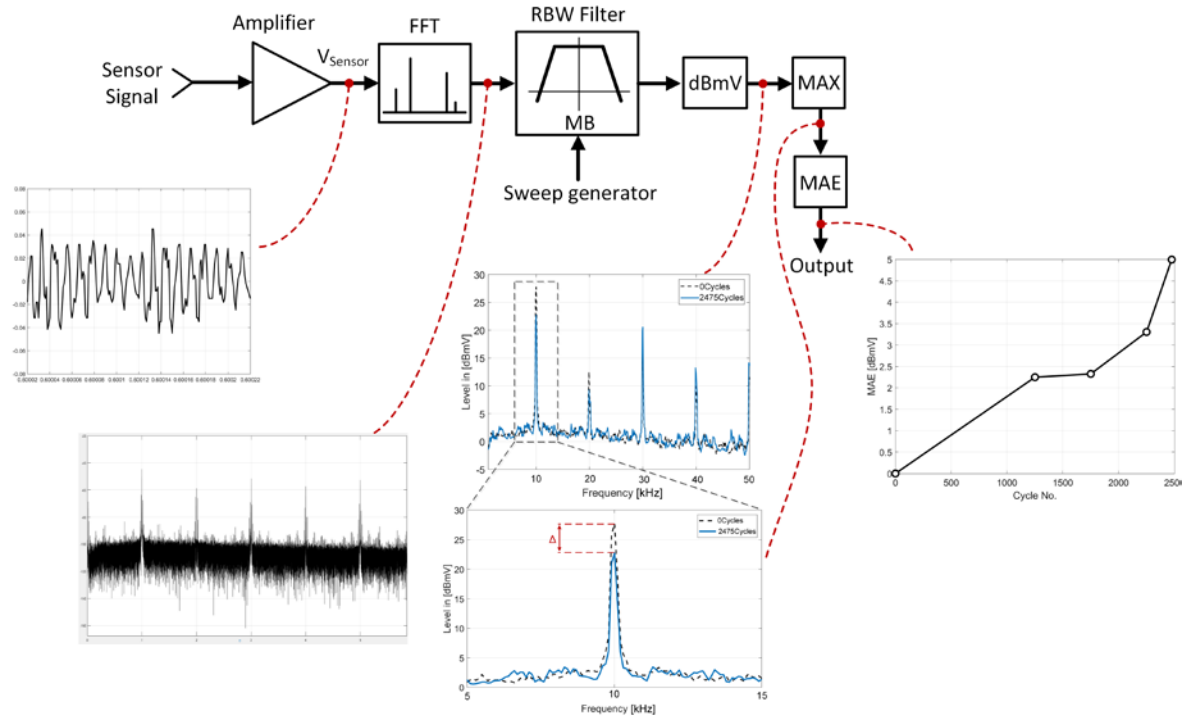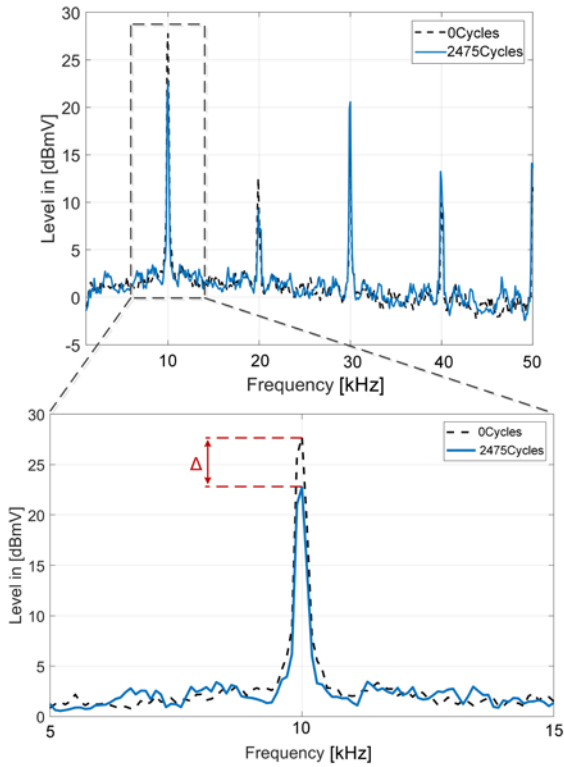*Figure 7. Top: comparison of spectrum analysis between fresh conditions (0 cycles) and end-of-test conditions (2475 cycles). Bottom: frequency zoom around 10 kHz.*

emission as a function of the aging.

At every measurement point, the module was cooled down to 23 °C to avoid the influence of temperature. This process was stopped at 2475 cycles, as the power module failed due to a gate breakdown at the upper switch of phase-leg C used for power cycling.

Figure 6 illustrates the conceptual schematic of the proposed measurement method. The *sensor signal* comes from the professional sensor as described in the previous section. After amplification in both cases, it is acquired from the oscilloscope (not illustrated) and processed with fast Fourier Transform (FFT). A Resolution Bandwidth Filter (RBW) is used as next stage to analyze frequency windows at variable Mid-Band (MB) or intermediate frequencies according with a sweep generator as presented in [16]. After that, a spectrum amplitude measurement is performed for the selected window and a maximum absolute error (MAE) is calculated in respect to the spectrum at initial conditions (fresh device), as follows:

$$MAE = \left| V_{sensor,nCycle}[dBmV] - V_{sensor,0Cycle}[dBmV] \right| \quad (1)$$

with obvious meaning of the quantities in the formula. The above procedure has been repeated for two modules at 10 kHz switching frequency.

It is worth to note that the above process has here been done offline by means of MATLAB software. Aiming at real application will require an audio processor, which is not in the purpose of this study.
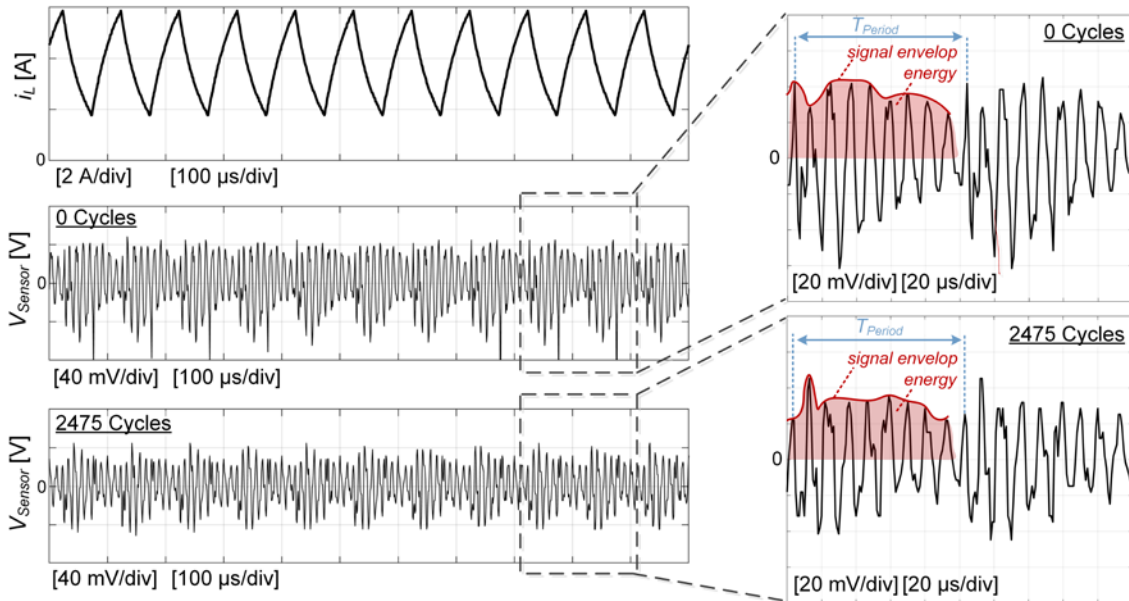

Figure 8. Time-domain waveforms of the acquired acoustic signal at 0 cycles (top) and 2475 cycles (bottom). A difference in the time-domain shape of a waveform period appears evidently if one consider a zoom on the time axis (right hand side). The change in energy (shaded area) is evident as well.

4. Results

Figure 7 shows the comparison between fresh conditions (0 cycles) and end-of-test conditions (2475 cycles) during switching operations at 10 kHz. In the bottom figure, a detail around 10 kHz is illustrated, clearly evidencing a decrease in the level amplitude related to power cycling.

Figure 8 exemplifies measured acoustic emissions with corresponding switched inductor current at 10 kHz in time domain. As it can be seen comparing 0 cycles and 2475 cycles measurements, the signal envelope is clearly different. This signal envelope contains signal characteristics such as period, energy (i.e., area under the envelope), amplitude and counts. Conventionally, these parameters have been used in order to differentiate and identify specific behavior of the device under test. However, an effective approach is to utilize frequency domain analysis as it was shown in Figure 7, which the signal salient features can be extracted more effectively from.

Figure 9a shows the evolution of MAE in respect to number of cycles. A positive trend can be clearly observed, showing that acoustic emission increases with number of cycles. The initial phase is clearly lacking of sampling point as we used very harsh accelerated conditions to speed up the test. A coherent trend can be observed on the on-state voltage drop shown in Figure 9b. On-state voltage drop is the reference quantity for degradation estimation, as an additional voltage drop appears at the bond wire interface with the die metallization when degradation takes place. The quantity on the second axis is calculated as the average on-state voltage drop Vce_{avg} measured during the on time of power cycling. Two comments are necessary about the measurement method, though. First, averaging has been necessary because on-state voltage Vce changes significantly as temperature does during the on time of power cycling. Second, all the measurements have been taken at a collector current $I_C = 45$ A, except the first one, as we mentioned before, as an increase in the acceleration factor has been needed to speed up the aging process. To take this discrepancy into account, a correction of the on-state voltage drop has been made on the first point only (0 cycles) according to the device datasheet, which yielded 2.82 V @ 45 A in respect to 2.33 V @ 35 A. It is worth to note, though, that regardless of the first point, the general Vce_{avg} trend is obviously coherent with the acoustic emission through MAE. This result is very promising and in our opinion gives a sound proof of concept of the proposed method.
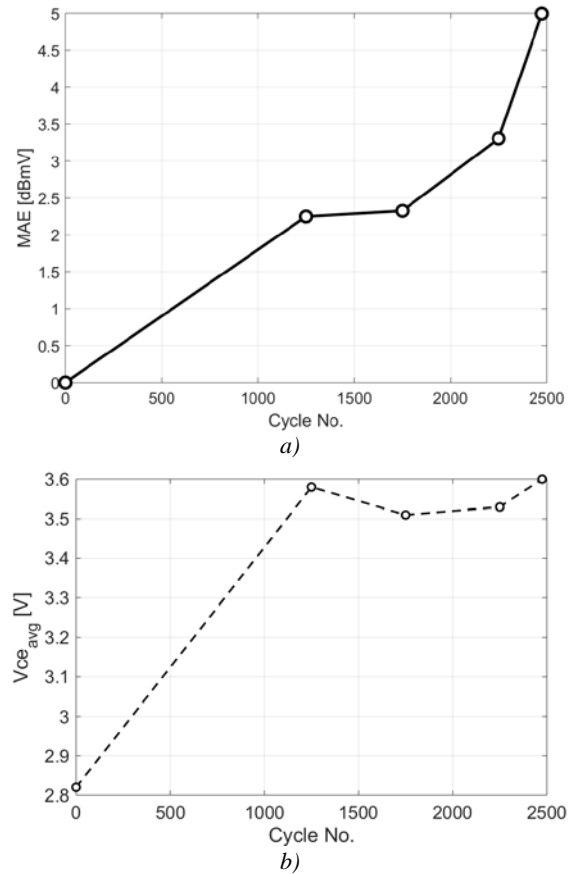

a)

b)

Figure 9. a) Evolution of maximum absolute error (MAE) and b) evolution of average Vce with respect to number of cycles (1st module under test).

5. Repeatability Test

In order to determine whether the drop in the acoustic emission can be used as reliable indicator, the same test has been performed on a second pristine module. The same parameters have been used as described in Section 4. For having comparable results, the number of cycles are kept the same, although this module did not fail after 2475 cycles. However, it is still to be considered aged due to the power cycling.

Tests on the second module have been performed in two phases. First, we turned on the measurement setup, including the acoustic sensor, but we did not perform any power cycling. At the same time instants of the first test, though, we briefly activated switching and performed acoustic acquisitions. To better fill the diagram, more points have been acquired, though. These results have been reported in Figure 10, where the equivalent number of cycles have been used in place of times, for the sake of comparison. Second, we performed power cycling in the identical conditions of the first module (see Figure 9a and b), and again
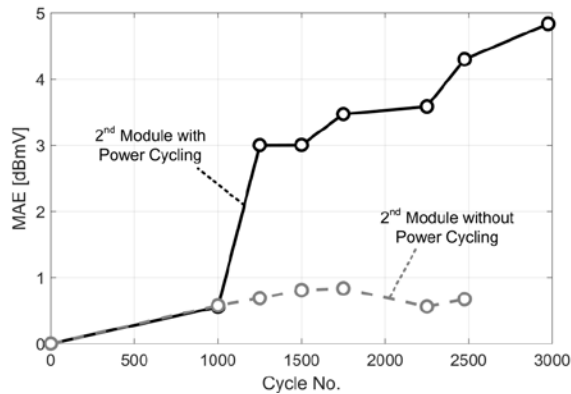
Figure 10. Behavior comparison in terms of acoustic emission before and after aging (2nd module under test).

performed acoustic acquisitions. The results have been reported in Figure 10 as well for the sake of comparison.

The obtained results displayed in Figure 10 show a remarkable difference between the case of no power cycling and the one with power cycling. The figure proves that no artifacts can come from the sensor heating or aging, as the acquisitions in case of no power cycling almost produce constant acoustic emission.

Figure 10 matches also very well the results of Figure 9 from the first module. The trend is very similar and the maximum absolute error at the end of the test, i.e. at 2475 cycles, is in very good agreement with the results of the first module, showing a strong repeatability of the results.

6. Conclusion

In this work, a novel method to detect aging through acoustic emission differences during real operation of a power module has been successfully presented and discussed. The correlation between acoustic emission and the degree of aging based on on-state voltage drop has been provided too, proving that it is possible to measure state of health by this method.

For the sake of completeness, repeatability tests have been performed, showing excellent correlation between the results obtained on two different samples of the same part number.

The proposed method presents disruptive qualities of non-invasiveness, i.e. is able to detect variation in the state of health without any contact with the active parts of the module. As unique disadvantage, the method is based on frequency-domain analysis, which has the intrinsic drawback of need for computational capacity. Nevertheless, implementation with simple audio processors, especially for near-real-time process can reasonably be consider for the purpose,

and will be the object of future work.

References

[1] L. M. Moore and H. N. Post, "Five years of operating experience at a large, utility-scale photovoltaic generating plant," *Prog. Photovoltaics Res. Appl.*, vol. 16, no. 3, pp. 249–259, May 2008.

[2] Reliawind, "Report on Wind Turbine Reliability Profiles – Field Data Reliability Analysis."

[3] S. Yang, A. Bryant, P. Mawby, D. Xiang, L. Ran, and P. Tavner, "An Industry-Based Survey of Reliability in Power Electronic Converters," *IEEE Trans. Ind. Appl.*, vol. 47, no. 3, pp. 1441–1451, 2011.

[4] U. M. Choi, F. Blaabjerg, and F. Iannuzzo, "Advanced power cycler with intelligent monitoring strategy of IGBT module under test," *Microelectron. Reliab.*, vol. 76–77, 2017.

[5] U. M. Choi *et al.*, "Power cycling test and failure analysis of molded Intelligent Power IGBT Module under different temperature swing durations," *Microelectron. Reliab.*, vol. 64, 2016.

[6] K. B. Pedersen, P. K. Kristensen, K. Pedersen, C. Uhrenfeldt, and S. Munk-Nielsen, "Vce as early indicator of IGBT module failure mode," in *2017 IEEE International Reliability Physics Symposium (IRPS)*, 2017, p. FA-1.1-FA-1.6.

[7] N. Baker, F. Iannuzzo, S. Munk-Nielsen, L. Dupont, and Y. Avenas, "Experimental Evaluation of IGBT Junction Temperature Measurement via a Modified-VCE (#x394;VCE_ #x394;VGE) Method with Series Resistance Removal," in *CIPS 2016; 9th International Conference on Integrated Power Electronics Systems*, 2016, pp. 1–6.

[8] A. Singh, A. Anurag, and S. Anand, "Evaluation of Vce at Inflection Point for Monitoring Bond Wire Degradation in Discrete Packaged IGBTs," *IEEE Trans. Power Electron.*, vol. 32, no. 4, pp. 2481–2484, Apr. 2017.

[9] S. Bęczkowski, P. Ghimre, A. R. de Vega, S. Munk-Nielsen, B. Rannestad, and P. Thøgersen, "Online Vce measurement method for wear-out monitoring of high power IGBT modules," in *2013 15th European Conference on Power Electronics and Applications (EPE)*, 2013, pp. 1–7.

[10] N. Baker, L. Dupont, S. Munk-Nielsen, F. Iannuzzo, and M. Liserre, "IR camera validation of IGBT junction temperature measurement via peak gate current," *IEEE Trans. Power Electron.*, vol. 32, no. 4, 2017.

[11] T. J. Kärkkäinen, J. P. Talvitie, M. Kuisma, P. Silventoinen, and E. Mengotti, "Measurement challenges in acoustic emission research of semiconductors," in *2015 17th European Conference on Power Electronics and Applications (EPE'15 ECCE-Europe)*, 2015, pp. 1–6.

[12] T. J. Kärkkäinen, J. P. Talvitie, M. Kuisma, P. Silventoinen, and E. Mengotti, "Acoustic emission caused by the failure of a power transistor," in *2015 IEEE Applied Power Electronics Conference and Exposition (APEC)*, 2015, pp. 2481–2484.

[13] T. J. Kärkkäinen, J. P. Talvitie, O. Ikonen, M.

Kuisma, P. Silventoinen, and E. Mengotti, "Sounds from semiconductors - Acoustic emission experiment with a power module," in *2014 16th European Conference on Power Electronics and Applications*, 2014, pp. 1–6.

[14] T. J. Kärkkäinen *et al.*, "Acoustic Emission in Power Semiconductor Modules—First Observations," *IEEE Trans. Power Electron.*, vol. 29, no. 11, pp. 6081–6086, 2014.

[15] S. Müller, C. Drechsler, U. Heinkel, and C. Herold, "Acoustic emission for state-of-health determination in power modules," in *2016 13th International Multi-Conference on Systems, Signals & Devices (SSD)*, 2016, pp. 468–471.

[16] P. Davari, E. Hoene, F. Zare, and F. Blaabjerg, "Improving 9-150 kHz EMI Performance of Single-Phase PFC Rectifier." 2018.